The microcalorimetry of lipid membranes

2004 J. Phys.: Condens. Matter 16 R441

(http://iopscience.iop.org/0953-8984/16/15/R01)

INSTITUTE OF PHYSICS PUBLISHING JOURNAL OF PHYSICS: CONDENSED MATTER

J. Phys.: Condens. Matter **16** (2004) R441–R467 PII: S0953-8984(04)59359-1

TOPICAL REVIEW

The microcalorimetry of lipid membranes

Heiko Heerklotz

Biozentrum of the University of Basel, Division of Biophysical Chemistry, Klingelbergstrasse 70, CH-4056 Basel, Switzerland

E-mail: heiko.heerklotz@unibas.ch

Received 14 January 2004
Published 2 April 2004
Online at stacks.iop.org/JPhysCM/16/R441
DOI: 10.1088/0953-8984/16/15/R01

Abstract

Insight into the forces governing a system is essential for understanding its behaviour and function. Calorimetric investigations provide a wealth of information that is not, or is hardly, available by other methods. This paper reviews calorimetric approaches and assays for the study of lipid vesicles (liposomes) and biological membranes. With respect to the instrumentation, differential scanning calorimetry (DSC), pressure perturbation calorimetry (PPC), isothermal titration calorimetry (ITC) and water sorption calorimetry are considered. Applications of these techniques to lipid systems include the measurement of thermodynamic parameters and a detailed characterization of the thermotropic, barotropic, and lyotropic phase behaviour. The membrane binding or partitioning of solutes (proteins, peptides, drugs, surfactants, ions, etc) can also be quantified. Many calorimetric assays are available for studying the effect of proteins and other additives on membranes, characterizing non-ideal mixing, domain formation, stability, curvature strain, permeability, solubilization, and fusion. Studies of membrane proteins in lipid environments elucidate lipid–protein interactions in membranes. The systems are described in terms of enthalpic and entropic forces, equilibrium constants, heat capacities, partial volume changes etc, shedding light also on the stability of structures and the molecular origin and mechanism of structural changes.

Contents

1. Introduction

Impressive progress has been made in detecting and imaging structural properties of biological systems. However, structure data are only a first step towards an understanding of physiological processes. Insight into the functions of biological macromolecules requires additional information on dynamics and on the interactions governing the behaviour. Such issues are tackled by bio-thermodynamics and calorimetry, and an increasing number of researchers recognize the great potential of these techniques. Excellent microcalorimeters and a broad variety of calorimetric techniques and assays have been developed over the last decade and are now available to a broad spectrum of users.

This article is mainly directed to researchers working in the field of lipid membranes in biological as well as model (e.g., vesicle) systems [1–3]. It aims at providing an overview of calorimetric techniques that have been used to study such systems. The broad scope of the review makes it impossible to explain the thermodynamic background or technical details of the methods (see, for example, [4–6]) or to discuss the results obtained by using them. Instead, the paper must be limited to making one aware of the calorimetric assays that are available to tackle a certain problem and to giving a few selected references.

One current trend in membrane calorimetry seems to be the consideration of increasingly complex systems. Vesicles of DMPC or DPPC (dimyristoyl- and dipalmitoylphosphatidylcholine) have yielded important information, but there are many other problems for which these lipids are rather poor model systems. The great interest in lipid rafts has led to a much broader consideration of complex mixtures of glycero-,

sphingo-, and glycolipids and sterols. The calorimetry of biological membrane extracts, viruses or whole cells is being further developed. Another important development is the ongoing introduction of new instruments, techniques and assays. For example, pressure perturbation calorimetry has recently been made available to users in the field [7]. It has already led to interesting results but its full potency for biophysical applications remains to be explored. Integrated circuit calorimetry is another promising new technique that allows for a miniaturization of the instruments and sample volumes, and provides fast response, relatively high sensitivity and great versatility at rather low cost [8].

The crucial challenge is to combine insights from biochemistry and physiology with those from structural biology and from bio-thermodynamics to derive an integral picture of membranes and their functions. Unfortunately, the recent success in tackling this problem is rather limited. Molecular dynamics simulations may be of great value to overcome the gap between the disciplines. Furthermore, substantial progress of both structural and thermodynamic insight will be required for deriving a general understanding of membranes and other systems.

2. Techniques

Calorimeters measure the heat consumed or released by a sample upon re-equilibration after a perturbation. Such perturbations can be caused by a change in temperature (DSC), addition of material (ITC), a change in pressure (PPC) or in water activity (sorption calorimetry). For a comparison between different types of calorimeters, such as adiabatic, heat flow, or power compensation instruments, see, for example, Wadsö's review [6]. Briefly, the fast response time of power compensation instruments makes them more sensitive for measuring the heats of fast effects and for revealing their kinetics. Heat flow calorimeters can provide a better long-term stability of the temperature and the baseline signal which is particularly important if slow processes are investigated.

2.1. Differential scanning calorimetry (DSC)

For a detailed introduction to DSC, see [9], an instrument is described in [10, 11]. Briefly, DSC records the temperature-dependent isobaric heat capacity, $C_p(T)$, of a sample:

$$C_p = \left.\frac{\partial H}{\partial T}\right|_p . \tag{1}$$

To this end, heaters at the sample and reference cell of the calorimeter are controlled by a feedback mechanism (i) to eliminate any temperature difference between the cells, and (ii) to increase the temperature of the two cells at a constant rate. An adiabatic shield kept at the same temperature as the cells prevents any heat exchange of the cells with the environment so that the heat uptake of the sample corresponds to the (known) electric power of the heater.

The raw signal represents the difference of C_p between the sample and buffer, which must be taken into account in determining absolute values of C_p [12]. In most cases, raw DSC curves are used to detect and quantify phase transitions using arbitrarily defined baselines, so the correction for the buffer is not required.

Equation (1) shows that the integral of a DSC curve from an appropriate base line yields the enthalpy change of the transition, ΔH. Different instruments allow one to study lipid vesicle suspensions in excess water, lipid samples of defined water content, or lipid suspensions at elevated pressure. Further to characterizing thermal transitions of lipids and proteins, DSC is also used to determine the amount of freezable water in order to study lipid hydration.

2.2. Isothermal titration calorimetry (ITC)

ITC is based on a series of (e.g., 20) consecutive injections of a liquid sample (a few μl each) from a syringe into the calorimeter cell under isothermal conditions. The heat of 'reaction' is measured as a function of the injection number, i.e. dependent on the concentration of the injectant in the cell. The reaction of the system may be transitions or transfers of molecules between different chemical or physical states. Considering that the injection causes ΔN^{trans} moles of a compound to undergo a transition that is accompanied by a molar enthalpy change of ΔH^{trans}, we may write the measured heat q as a sum over the enthalpy changes of all i processes induced by the injection:

$$q - q_{\text{dil}} = \sum_i \Delta N_i^{\text{trans}} \Delta H_i^{\text{trans}}. \tag{2}$$

The term q_{dil} denotes heats of dilution that occur due to changes in intermolecular (or interparticle) interactions of the injectant and of the cell content. These effects are determined by blank runs injecting the titrant into buffer (and buffer into the cell content) and are eliminated by subtracting the resulting heats. It should however be noted that it is not always possible to perform a blank experiment that measures the heats of dilution in the absence of other heat effects. It can therefore be advantageous to treat q_{dil} or Q_{dil} (see below) as a constant, adjustable parameter in the data evaluation [13].

It is often convenient to work with normalized differential heats, Q, which are given per mole of titrant injected, ΔN^{inj}. For the case that only one heat-producing (or consuming) process occurs ($i = 1$), we find

$$Q - Q_{\text{dil}} = \frac{q - q_{\text{dil}}}{\Delta N^{\text{inj}}} = \frac{\Delta N^{\text{trans}}}{\Delta N^{\text{inj}}} \Delta H^{\text{trans}} = \frac{\Delta C^{\text{trans}}}{\Delta C^{\text{inj}}} \Delta H^{\text{trans}}. \tag{3}$$

Equation (3) illustrates that one may replace a ratio of mole numbers, N, in a common volume (the calorimeter cell) by a ratio of molar concentrations, C. The expression ΔC^{trans} specifies the moles per cell volume that undergo the heat-producing transfer or transition, and ΔC^{inj} denotes the change in the concentration of the injectant in the cell caused by the injection.

To evaluate ITC curves, one has to derive a model for the process under investigation that relates ΔN^{trans} to the total concentrations of all compounds in the cell (known) and one or two adjustable parameters (usually including an equilibrium constant). Different types of assays can be performed.

(i) *Reaction assays* study interactions between two compounds (one originally loaded into the cell and the other into the syringe) by bringing them in contact with each other in the cell. A binding assay can be used to determine the equilibrium constant (as described by the mass action law) and ΔH. The uptake protocol for membrane partitioning serves to determine the membrane–water partition coefficient, K, and ΔH.

(ii) *Dilution assays* are based on injections of a sample into a large excess volume of water or buffer. Bimolecular interactions between molecules (or particles such as vesicles) in solution give rise to heats of dilution that depend only slightly on concentration, i.e., ITC curves are constant or decrease gradually during the titration. Such experiments are often performed as 'blank' measurements to correct other data sets (e.g., partitioning curves) for dilution effects. If oligomers or micelles (demicellization assay) are diluted into water, one obtains more cooperative dissociation curves that allow one to determine the equilibrium constant K or critical micelle concentration (CMC), and the enthalpy change of demicellization, $\Delta H_S^{\text{m}\to\text{w}}$ (read: the change, Δ, in molar enthalpy, H, of the solute, S, upon transfer from micelles, m, to water, w). The release assay serves to characterize membrane partitioning of solutes by injecting solute-containing vesicles into water/buffer.

(iii) *Partial enthalpy assays* are performed under conditions ensuring that all injected material undergoes a certain transition, i.e., $\Delta C^{\text{trans}} = \Delta C^{\text{inj}}$. Then, the normalized heat, $Q - Q_{\text{dil}}$, equals the partial molar enthalpy change, ΔH^{trans}. For membrane partitioning, this condition is realized at lipid concentrations, C_{L}, that are large compared to the 'dissociation constant', $C_{\text{L}} \gg K^{-1}$ (see equation (8)). Such experiments are performed in order to obtain independent information on the molar enthalpy change of solute transfer from water into bilayers, $\Delta H_{\text{S}}^{\text{w}\to\text{b}}$ (see section 4.2, figure 8). Concentration-dependent enthalpies of membrane insertion can also be interpreted in terms of non-ideal lipid–solute mixing thermodynamics and show sudden changes at solute-induced phase transitions (see section 5, figure 9).

Generally, the calculation of the concentrations of the pre-loaded and injected substances in the cell has to take into account the design of the instrument. If the calorimeter works with completely filled cells that overflow when material is added, proper corrections must be applied, which are not discussed in this general review.

2.3. Pressure perturbation calorimetry (PPC)

Different calorimeters have been designed for the measurement of the heat accompanying an isothermal pressure change, $\mathrm{d}Q/\mathrm{d}p|_T$. Such techniques have been referred to as, e.g., piezothermal analysis [14], scanning transitiometry [15, 16], pressure jump calorimetry [17, 18] or pressure perturbation calorimetry (PPC), [7]. A related, adiabatic technique has been termed volume perturbation calorimetry [19–22].

PPC is mainly used to determine the temperature-dependent, isobaric volume expansion of a sample, $\partial V/\partial T|_p$. This approach is based on the Maxwell relation of the reversible heat exchange upon a change in pressure, $\partial Q_{\text{rev}}/\partial p$ at constant temperature, T, to the temperature-induced volume change, $\partial V/\partial T$, at constant pressure, p:

$$\left.\frac{\partial Q_{\text{rev}}}{\partial p}\right|_T = -T\left.\frac{\partial V}{\partial T}\right|_p. \tag{4}$$

Over many years, mainly bulk liquids or solutions were studied on home-built, heat flow calorimeters, mostly using high pressures. Recently, a new generation of PPC instruments has become commercially available as an accessory to highly sensitive scanning calorimeters of the power compensation type [7]. The measurement is illustrated in figure 1. The extremely high sensitivity of the calorimeter makes it possible to study changes in the partial volume of as little as $\approx$1 mg of a protein using only very small pressure jumps of 5 bars. Randzio [24] has recently questioned the precision of this instrument, but he did not provide any quantitative arguments to substantiate his claims, and closer inspection shows that they are all irrelevant (see appendix B).

The first applications of the technique to lipids were studies of the kinetics of phase transitions on the basis of the relaxation of the temperature or heat changes following a pressure variation (see section 7). Volumetric investigations were performed characterizing lipid melting [23, 25] (see figure 4) and domain formation in membranes [26].

2.4. Water sorption calorimetry

Different calorimetric techniques have been applied to characterize the enthalpy and free energy of water binding to hygroscopic materials. All instruments have in common that a lipid film deposited on the wall of the cell is exposed to an atmosphere of varying water vapour activity (the relative humidity, RH). An increase in the humidity of the gas gives rise to an exothermic

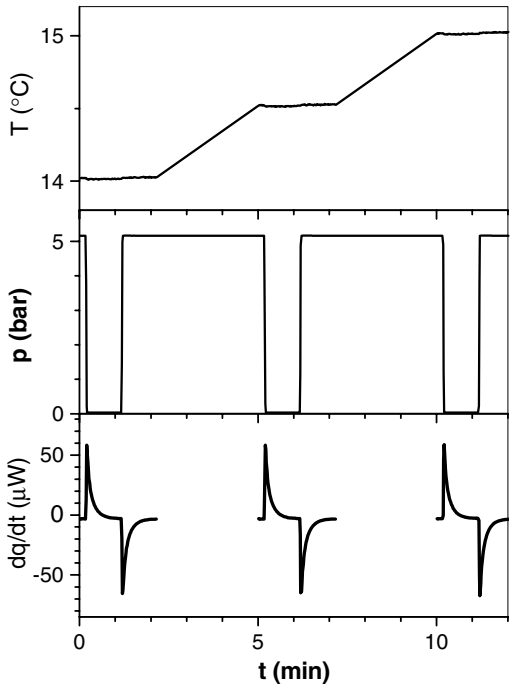

Figure 1. Detail of a PPC experiment with DMPC vesicles: Pressure (p) jumps between ambient pressure and 5 bar (above ambient) are applied to sample and reference cells and the temperature, T, is kept constant by a feedback heater. The power of the heater, $\mathrm{d}q/\mathrm{d}t$, is recorded (bottom panel) and integration of the peaks yields the isothermal heat response, $\mathrm{d}Q/\mathrm{d}p|_T$. The heat response is measured twice (after a down- and an up-jump in p) and then the instrument is automatically equilibrated at the next desired temperature (three out of typically 50 scheduled temperature points are shown). Reproduced with permission from [23], ©2002 American Biophysical Society.

heat that depends on the molar enthalpy of adsorption from vapour, $\Delta H_{\mathrm{W}}^{\mathrm{vap}\to\mathrm{b}}$, and the mole number of adsorbed water molecules, $\Delta N_{\mathrm{W}}^{\mathrm{vap}\to\mathrm{b}}$:

$$q = \Delta N_{\mathrm{W}}^{\mathrm{vap}\to\mathrm{b}} \Delta H_{\mathrm{W}}^{\mathrm{vap}\to\mathrm{b}}. \tag{5}$$

The adsorption of vapour to the membrane is exothermic ($\Delta H_{\mathrm{W}}^{\mathrm{vap}\to\mathrm{b}} < 0$) since it includes (i) the enthalpy of condensation of water, $\Delta H_{\mathrm{W}}^{\mathrm{vap}\to\mathrm{liq}} = -40.6$ kJ mol^{-1}, and (ii) a (much smaller) enthalpy of binding of liquid water to the bilayer, $\Delta H_{\mathrm{W}}^{\mathrm{liq}\to\mathrm{b}}$:

$$\Delta H_{\mathrm{W}}^{\mathrm{liq}\to\mathrm{b}} = \Delta H_{\mathrm{W}}^{\mathrm{vap}\to\mathrm{b}} - \Delta H_{\mathrm{W}}^{\mathrm{vap}\to\mathrm{liq}}. \tag{6}$$

With the approximation $\Delta H_{\mathrm{W}}^{\mathrm{vap}\to\mathrm{b}} \approx -41$ kJ mol^{-1}, one can derive an estimate of $\Delta N_{\mathrm{W}}^{\mathrm{vap}\to\mathrm{b}}$ directly from q using (5). The *sorption curve*, $N_{\mathrm{W}}^{b}(\mathrm{RH})/N_{\mathrm{L}}$, is obtained by integration of q over RH and normalization with respect to the mole number of lipid, N_{L}. In order to explore the mechanism of water binding in terms of $\Delta H_{\mathrm{W}}^{\mathrm{liq}\to\mathrm{b}}$, it is necessary to determine q and $\Delta N_{\mathrm{W}}^{\mathrm{vap}\to\mathrm{b}}$ independently. Different techniques have been described to generate well-defined RH variations in a calorimeter and to measure q and $\Delta N_{\mathrm{W}}^{\mathrm{vap}\to\mathrm{b}}$.

Bakri's [27] instrument perfuses the sample in the calorimeter cell with a gas stream of variable humidity that is adjusted by mixing dry and water-saturated gas (at the experimental temperature T_0) in varying proportions. Then, the gas flow enters the sample cell. After an increase in RH, some water molecules are adsorbed so that a heat q is released and the RH of

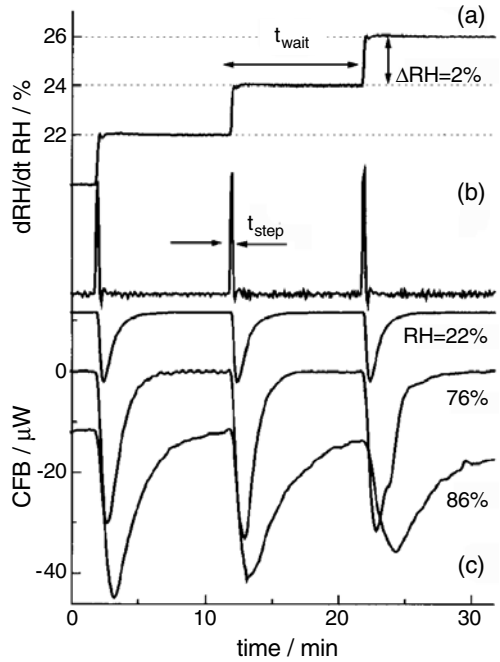

Figure 2. Detail of a sorption calorimetry experiment with POPC using the humivar technique. The sample is perfused with moist nitrogen with a relative humidity, RH, varied in steps of 2% every 10 min. The change in RH, $\mathrm{dRH}/\mathrm{d}t$, induces the adsorption of water molecules to the lipid. This gives rise to an exothermic heat effect that is detected as a transient decrease of the power of the cell feedback heater (CFB). Reproduced with permission from [28], ©1999 by Academic Press.

the gas flow leaving the cell is transiently reduced. After leaving the sample cell, the gas flow is led into a second calorimeter cell containing water, where its RH is brought to 100% by evaporation. The accompanying heat is proportional to (100%-RH), so the RH of the incoming flow and, in particular, the 'lacking' water that was adsorbed by the lipid, $\Delta N_{\mathrm{W}}^{\mathrm{vap}\rightarrow\mathrm{b}}$, can be independently quantified.

Binder *et al* [28, 29] have developed a device named 'humivar' [30], providing a gas flow of well-defined humidity by adjusting the temperature T of an evaporator unit to a value below the experimental temperature, T_0. Upon heating to T_0, the RH decreases from $\mathrm{RH}(T) = 100\%$ to $\mathrm{RH}(T_0) < 100\%$. The instrument software allows one to run a 'humidity staircase', $\mathrm{RH}(t)$, with precise steps in RH (e.g., by 2%) after defined time intervals (see figure 2). Thus, one can automatically scan virtually the whole RH range, up and down, with high resolution. The gas flow is led into an isothermal calorimeter where q is measured. The sorption curves, (the number of bound water molecules per lipid, $R_{\mathrm{W/L}}$, as a function of RH), are determined gravimetrically.

Smith [31, 32] has included a quartz microbalance within a calorimeter cell so that the gravimetric measurement of the sorption curve, $R_{\mathrm{W/L}}(\mathrm{RH})$, and the calorimetric measurement of the sorption heat, $q(\Delta\mathrm{RH})$, can be done simultaneously.

Markova *et al* [33, 34] have built a closed system with an evaporation cell and a sorption cell in separate calorimeter channels connected by a thin steel tube. After opening the tube, water vapour diffuses slowly to the sample, and the two channels measure the heat of evaporation (yielding $\Delta N_{\mathrm{W}}^{\mathrm{vap}}(t)$) and the heat of sorption, $q(t)$, so that the molar heat of sorption can be computed.

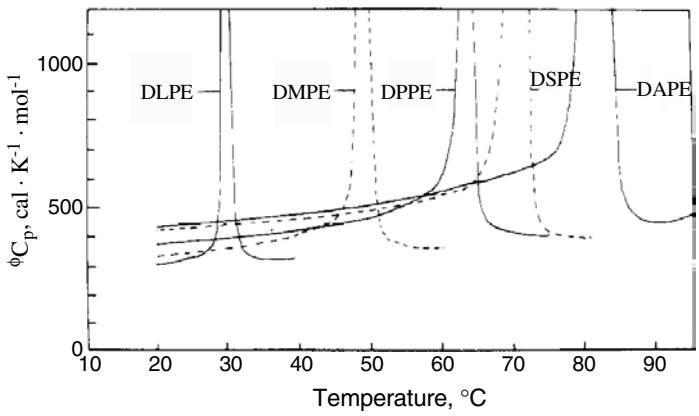

Figure 3. Apparent molar heat capacities of membranes of a series of 1,2-diacyl-sn-glycero-3-phosphoethanolamine (DXPE) with X = lauryl (L), myristoyl (M), palmitoyl (P), stearoyl (S) and arachidoyl (A). Both the heat capacity of the lipids and the melting temperature increase with increasing chain length. Reproduced with permission from [12], ©1983, American Chemical Society.

3. Applications to lipid systems

3.1. Properties of liquid-crystalline membranes

Thermodynamic parameters of membranes in a certain state that can be measured calorimetrically are, in particular, the isobaric heat capacity and the thermal volume expansion. Absolute heat capacities of different lipid bilayers were determined by Blume [12] using DSC. He found that C_p depends strongly on the head group and chain length (see figure 3) and the contribution per methylene group in most lipids is larger than in alkanes. The results were discussed in terms of contributions of hydrophobic hydration of the lipid tails to C_p.

The thermal *volume expansion* coefficient of fluid membranes is typically about 10^{-3} K^{-1}, and it can be precisely and conveniently measured by PPC [23]. The method determines the volume changes by applying small pressure jumps that apply homogeneously to the whole sample. The reduction of the partial volume of the lipid in the membrane that is induced by an increase in pressure is highly anisotropic. Since more ordered chains can be packed more tightly together, a reduction of the volume is accompanied by a lateral area condensation but an increase in membrane thickness.

The heat accompanying an *area change* of the membrane can be measured by ITC experiments injecting vesicles into a hypo- or hyperosmotic solution [35]. The osmotically driven uptake of water into the interior of the vesicles induces an elastic lateral stretching of the membrane which is endothermic. Lateral compression of the membrane in a hyperosmotic environment is exothermic. Since the area, volume and thickness of the bilayer are coupled with each other (see above), the data are closely related to those obtained by PPC.

3.2. Thermotropic phase behaviour of lipids and lipid mixtures

Lipids can form a large variety of phase structures as a function of the chemical composition (including length and unsaturation of the chains), temperature, pressure (see below), hydration, etc. Typical phases at low temperature are bilayers in different subgel, gel, and ripple phases. These phases have stretched acyl chains (i.e., in all-trans conformation) giving rise to wax-like

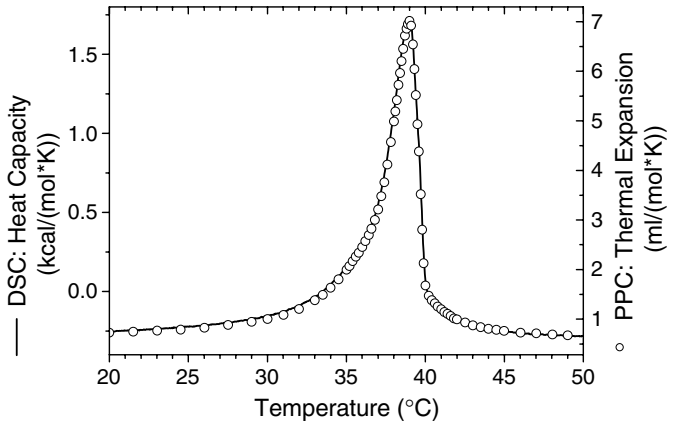

Figure 4. Comparison of the DSC (line, left-hand axis) and PPC (○, right-hand axis) curves at the chain melting transition of egg sphingomyelin. Integration of the peaks yields $\Delta H = 7.3$ kcal mol^{-1} (DSC) and $\Delta V = 21$ ml mol^{-1} (PPC). Reproduced with permission from [26], ©2002 American Biophysical Society.

properties. At the main transition or melting temperature, T_m, the ordered phase is transformed into the liquid crystalline (or fluid) phase. At even higher temperature, certain lipids form inverse hexagonal or cubic phases.

Since the pioneering studies of Chapman [36, 37] and others, the standard technique to monitor these phase transitions is DSC. Pure lipids usually have very sharp melting transitions with halfwidths of the order of 0.05 K. Since impurities tend to broaden the transition, the width can be considered an indicator of purity. Strong membrane curvature in small vesicles as well as undulations or shape fluctuations of large unilamellar vesicles also broaden the transition, and may slightly shift its maximum to lower temperature. Over the years, a wealth of lipid melting data has been collected and the effects of chain length and unsaturation, head group and backbone structure, etc on T_m and ΔH have been thoroughly studied and modelled. For extensive reviews of phase transitions in different lipid classes, see Koynova and Caffrey's reviews on glycerolipids [38], phosphatidylethanolamines [39], sphingolipids [40] and phosphatidylcholines [41] and the lipidat data bank [42].

Recently, PPC (see above) has become commercially available as another tool to detect lipid melting, which is accompanied by a peak in thermal expansivity. Interestingly, the PPC and DSC peaks of lipid melting (see figure 4) exhibit almost perfectly the same shape [23, 25, 26], suggesting that both the enthalpy and volume of the membrane are governed by the same molecular parameter, most likely the abundance of gauche isomers in the chains. For a more sophisticated discussion of the phenomenon, see [25]. The increase in partial volume of lipid bilayers upon chain melting is of the order of 3% [23, 25, 43].

Interestingly, many phospholipids with saturated chains of various lengths share the same pressure dependence of the phase transition, $dT_m/dp \approx 20$ K kbar^{-1} (see section 3.3), suggesting that this is an intrinsic property of the trans–gauche isomerization of the chains. Hence, inspection of this parameter could serve to distinguish chain melting transitions from others. This parameter can be determined from a series of DSC scans at various pressures (yielding $T_m(p)$), or by comparing ΔV and ΔH obtained by PPC and DSC according to the Clausius–Clapeyron equation:

$$\frac{dT_m}{dp} = \frac{\Delta V}{\Delta S} = T_m \frac{\Delta V}{\Delta H}. \tag{7}$$

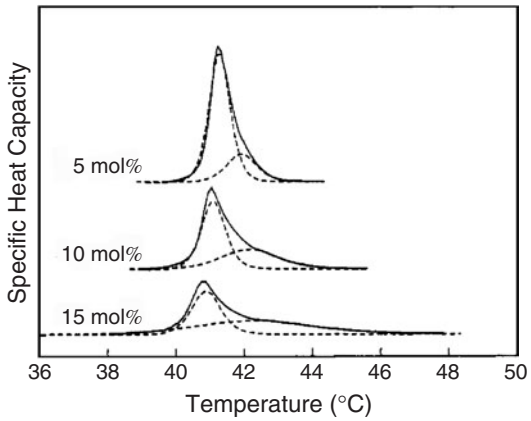

Figure 5. DSC curves of DPPC containing various amounts of cholesterol as indicated in the plot. The dotted curves illustrate the deconvolution into two components. The maximum position and the width of the overall peak depend on the position and shape of the two components in a complex manner, so care must be taken to avoid misinterpretations [46, 47]. Reproduced with permission from [46], ©1993 American Chemical Society.

Equation (7) can also be used to compute ΔV from pressure-dependent measurements of T_m using DSC [19, 22, 23].

Lipid mixtures can show a very complex thermotropic phase behaviour including eutectic or peritectic points or compound formation; for excellent overviews, see Lee [44] and Cevc and Marsh [1]. DSC is the standard method to establish phase diagrams by detecting the onset and completion of thermotropic phase transitions. More sophisticated studies have modelled the complete DSC peak, yielding not only transition temperatures but also thermodynamic non-ideality parameters describing the interactions in the mixture [45].

Sterols such as cholesterol can split the melting transition of phospholipid membranes into a sharp and broad component, suggesting a gradual de-mixing of the membrane (see figure 5). A proper deconvolution may be important for a correct interpretation of the phase behaviour [46–51]. The characterization of mixing thermodynamics by ITC as outlined in section 5.1 is, unfortunately, not applicable to phospholipid mixtures, since the exchange of lipid molecules between vesicles is too slow.

3.3. Barotropic phase behaviour

The fact that at least some lipid phase transitions are accompanied by substantial volume changes implies the existence of pressure-induced phase transitions (for an overview, see [52]). The sensitivity of a phase transition to pressure can be quantified in terms of the pressure-induced shift of the transition temperature, dT_m/dp, or the volume change of the transition, ΔV. Both parameters can be converted into each other according to equation (7), using ΔH measured by DSC. Shifted transition temperatures of lipids under elevated pressure have been measured by DSC using pressures ranging from 5 bar to kilobars [23, 25, 53, 54], yielding $T_m(p)$ and dT_m/dp. Differential or complete phase changes of samples have also been induced by pressure jumps at constant T (PPC, pressure calorimetry) [23, 25], yielding ΔV of the transition.

An increase in pressure can induce a transition from an inverse hexagonal to a fluid lamellar phase ($dT_{hex}/dp \approx 40$ K kbar^{-1} [54]), the freezing of the fluid-lamellar to a ripple

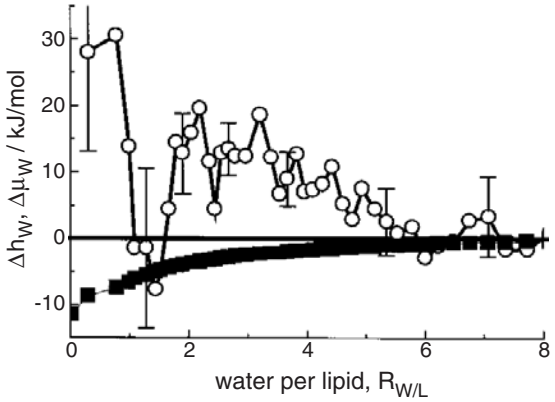

Figure 6. Enthalpy and chemical potential changes upon adsorption of liquid water to DOPC (in the notation used here, $\Delta H_W^{liq\rightarrow b}$ (○) and $\Delta \mu_W^{0,liq\rightarrow b}$ (■)). Reproduced with permission from [29], ©1999 by Elsevier Science B.V.

phase (≈20 K kbar^{-1} for saturated chains [23, 25, 53–55], and ≈14 K kbar^{-1} for DOPE [54]) and the pre-transition from the ripple to the lamellar gel phase (≈10–15 K kbar^{-1}, [23, 25, 55]).

3.4. Lipid hydration and lyotropic phase behaviour

The interactions of the polar and apolar parts of the lipids with water are the driving force for the formation of the different phases. Several calorimetric techniques quantify the interaction of water with lipids under different conditions and allow characterizing hydration phenomena in detail.

Water sorption calorimetry determines the enthalpy and entropy of water binding at a given temperature as a function of water activity. It has recently provided valuable insight into the molecular origin of the so-called hydration force, which causes a strong, short-range repulsion between two hydrated (bilayer) surfaces [56, 57]. The ordering of water molecules by lipid–water and water–water interactions as well as entropy gains arising from fluctuations in membrane structure were discussed as the basis of hydration forces. Sorption calorimetry showed for DOPC bilayers at 25 °C that only one or two water molecules per lipid exhibit an exothermic binding, i.e., these are bound by a specific interaction and are thus ordered. The attraction of the remaining ten or more water molecules adsorbed per lipid is endothermic and is therefore driven exclusively by a gain in entropy (see figure 6). Hence, water is bound to the lipid in order to increase its motional and conformational freedom, and the resulting entropy gains must also be considered the basis of the hydration force, at least under the conditions of the measurement. This important conclusion was further supported by sorption calorimetric studies of POPC [28] and a series of saturated lipids (3–4 enthalpically bound water molecules per lipid) [33].

The thermodynamics of a lyotropic gel-to-liquid crystalline transition of POPC at ≈40% RH have also been discussed on the basis of sorption calorimetry [28]. The enthalpy change accompanying a lyotropic lamellar-to-hexagonal transition depends on whether the lipid forms direct hydrogen bonds or not [58].

Another approach for determining the hydration pressure of lipid phases is to record the phase transition temperatures at different, well-defined water contents by DSC [59].

Finally, a characteristic number of lipid-bound water molecules, so-called ‘unfreezable water’, can be deduced from the enthalpy of water freezing/melting of a sample of well-defined water content [60–62].

3.5. Self-association of lipids

Typical membrane lipids have critical association concentrations in the nanomolar range which are not accessible by the ITC self-association protocol. Systematic studies have, however, been performed on short-chain diacylphosphatidylcholines and lysophosphatidylcholines [63]. The results were discussed in terms of group contributions to the enthalpy and free energy of self-association and changes in the water-accessible surface area (ASA) of lipids. Furthermore, they showed that the alignment of the acyl chains in an aggregate gives rise to a significant change in enthalpy (but not in free energy) compared to the state in bulk hydrocarbon. This finding is also important for the interpretation of enthalpies of insertion of molecules into lipid membranes.

4. Membrane partitioning and binding of additives

4.1. Specific binding of ligands to lipids and membrane receptors

ITC has become a standard method for characterizing ligand binding [64]. For this assay, a solution of a compound A filled into the cell is titrated with a solution of compound B loaded into the syringe. The equilibrium binding constant and enthalpy of the reaction are determined.

The change in the concentration of the product, ΔC^{trans}, that is caused by a change in the concentration of the injectant, $\Delta C^{\text{inj}} = \Delta C_{\text{B}}$ (see equation (3)) is derived on the basis of the mass action law. As a result, a model equation is obtained that allows one to fit the binding constant, K, the molar enthalpy change, ΔH, and the stoichiometry of the reaction to the ITC curve.

This model is appropriate for the binding of ligands to receptors residing in the membrane (e.g., [65]). Specific binding of ligands to lipids *per se* is however rare. It has recently been described for a drug, cinnamycin, binding to phosphatidylethanolamine [66]. In some cases, the mass-action model has been fitted to data observed upon unspecific partitioning of solutes into membranes showing a saturation behaviour due to non-ideal interactions or electrostatic effects. In this case, the physical meaning of the parameters is questionable, and more appropriate models should be preferred.

If lipids or membrane proteins in vesicles are concerned and the ligand is not able to permeate the membrane sufficiently quickly, the lipid/protein concentration must be corrected to include only the accessible part [65]. Different rather specific solutions to this problem have been described [65, 67]. A rather general method for testing whether or not the ligand permeates the membrane is based on a combination of ITC uptake and release experiments [68] as explained in section 4.2 and figure 7.

The protonation effects accompanying an enzymatic reaction were quantified by measuring reaction enthalpies in various buffers (see [69], see section 4.3).

4.2. The partitioning of non-ionic solutes into membranes

Solute partitioning into membranes can be studied very favourably by different types of ITC assays. The process giving rise to the heat Q is the transfer of solute (S) molecules from water (w) into the lipid bilayer (b), which is accompanied by a molar enthalpy difference, $\Delta H_{\text{S}}^{\text{w}\to\text{b}}$, or the release of solute from the bilayer membranes, accompanied by an enthalpy change $\Delta H_{\text{S}}^{\text{b}\to\text{w}} = -\Delta H_{\text{S}}^{\text{w}\to\text{b}}$. Hence, ΔC^{trans} in equation (3) has to be replaced by the change in the concentration of bilayer-bound solute, $\Delta C_{\text{S}}^{\text{b}}$. An expression for $\Delta C_{\text{S}}^{\text{b}}$ can be derived on the basis of a partition coefficient, K. A variety of definitions have been used for the partition coefficient; for a detailed discussion, see [70]. A good description of the partitioning

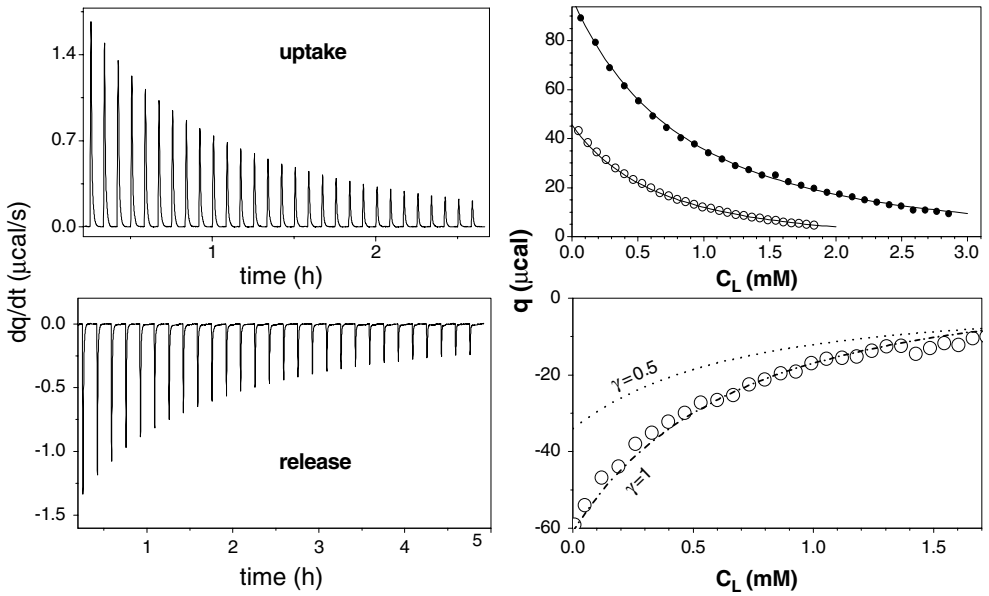

Figure 7. ITC uptake and release experiments. The left panels show the heat peaks after consecutive injections of 10 mM POPC vesicles into a 150 μM solution of the surfactant $C_{10}EO_7$ (uptake) and of mixed vesicles (10 mM POPC +1 mM $C_{10}EO_7$) into buffer (release). The corresponding integrated heats q are shown in the right-hand panels (○); an additional data set is shown for another experiment (14.8 mM POPC into 250 μM $C_{10}EO_7$, ●). A model based on equation (9) was fitted globally to the uptake data to determine K and $\Delta H_S^{w\to b}$ assuming either all or half of the bilayer to be accessible (i.e. the membrane being impermeable or permeable to the solute) (the solid curves of both fits are identical but correspond to different values of K). The results of the release experiment (bottom right-hand panel) were predicted from the parameters of the uptake experiments assuming permeable (– · – · –) and impermeable (· · · · · ·) membranes. The experimental data agree well with the prediction for permeable membranes.

of amphiphiles is often possible in terms of a constant mole ratio partition coefficient, K:

$$K = \frac{C_S^b}{C_L C_S^w} = \frac{C_S^b}{C_L\left(C_S - C_S^b\right)}. \tag{8}$$

The symbols C_L, C_S^b, C_S^w denote the molar concentrations of the lipid (L, virtually completely located in lipid bilayers), and of the solute (S) in bilayers (b), water (w), and total (no superscript).

Most ITC partitioning assays are based on injections of lipid vesicle suspensions into the cell. For the uptake protocol [71–74] (see upper panels of figure 7), the cell contains the solute in water/buffer so that every aliquot of lipid vesicles injected into the cell binds part of the remaining free solute. The release protocol [26, 68, 75] (see bottom panels of figure 7) is based on small injections of lipid bilayer vesicles containing solute into a large excess volume of buffer; the dilution gives rise to a release of solute from the bilayers.

A model equation that allows one to fit release ($C_S^{ini} = 0$) and uptake ($R^{syr} = 0$) data simultaneously is derived in appendix A, resulting in

$$Q = K\left[\frac{\left(C_S^{ini} + R^{syr}C_L\right)}{(1 + KC_L)^2} - \frac{R^{syr}\left(C_L^{syr} - C_L\right)}{\left(1 + KC_L^{syr}\right)(1 + KC_L)}\right]\Delta H_S^{w\to b} + Q_{dil}. \tag{9}$$

If only uptake data are evaluated, equation (9) simplifies to

$$Q = K\frac{C_S^{ini}}{(1+KC_L)^2}\Delta H_S^{w\to b} + Q_{dil}. \tag{10}$$

Note that the second, negatively signed term in the bracket of equation (9) vanishes for the uptake assay but is dominating in the release experiment, so that both protocols give rise to heats Q with opposite sign (see figure 7).

Another protocol determines the free solute concentration, $C_S^{w,syr}$, in a vesicle suspension by injecting an S–L mixture into water containing solute at different concentrations, C_S^{ini} [76, 77]. The heats obey the model given by equation (21) but instead of a fit, the assay is based on a series of experiments in order to find a C_S^{ini} giving rise to neither uptake nor release, $Q = Q_{dil}$, which occurs for $C_S^{ini} = C_S^{w,syr}$. Having identified C_S^w in a mixture of known C_S and C_L one may calculate $C_S^b = C_S - C_S^w$ and, in turn, K according to equation (8).

An extraction assay has also been based on injections of water into a solute-containing vesicle dispersion [78].

Although uptake and release assays serve to determine the same parameters, they are not redundant. Instead, a combination of the two protocols can resolve a number of issues and help to recognize and avoid errors and artefacts. One important point is that *membrane-impermeable solutes* can bind only to the outer leaflet of the vesicles, i.e., to a fraction $\gamma = 0.5$ of the lipid for large and $\gamma = 0.6$ for small unilamellar vesicles. If this is not taken into account, K is underestimated by a factor of two. To do so, one has to replace the lipid concentration used in the fit routine by γC_L. The crucial point of combining uptake and release assays is that C_S^{ini} and $R^{syr}C_L$ are no longer equivalent. Whereas all solute C_S^{ini} in the uptake experiment is free to partition between water and γC_L of the lipid, half of the pre-bound solute in the release experiment is entrapped in the inner leaflet of the vesicle and cannot be released. Thus, the correction $C_L \to \gamma C_L$ applied to equation (18) also yields the correct effective solute concentration, $C_S \to C_S^{ini} + R^{syr}\gamma C_L$. A consistent fit of uptake and release data with the same K and $\Delta H_S^{w\to b}$ is only possible if the correct value is used for γC_L, respectively, so that a wrong assumption regarding γ can be ruled out (bottom right-hand panel in figure 7).

Slow kinetics of membrane-uptake of the solute lead to heats of transfer vanishing in the baseline signal, an effect that may not be visible in the ITC curve, in particular in the case of complex kinetics. As a consequence, the extent of membrane uptake and thus K may be underestimated. Slow release kinetics would, however, mimic a higher affinity to the membrane so that K is overestimated. Again, the problem becomes obvious if uptake and release are combined.

The model (21) assumes that K and $\Delta H_S^{w\to b}$ are constant. In many cases, the *solute mixes non-ideally* with the lipid (see section 5.1) and these assumptions are not *a priori* warranted. Refined models allowing for composition-dependent K or $\Delta H_S^{w\to b}$ have been used [67, 79], but in most cases the experimental data do not justify the introduction of another adjustable parameter (such as a non-ideality parameter). However, it must be noted that the two-parameter model, equation (9), is quite robust, and yields good data even if the model assumptions are not strictly fulfilled. We have, for example, simulated data sets as obtained by ITC uptake experiments on the basis of a constant K and variable $\Delta H_S^{w\to b}$ changing from 26 to 32 kJ mol^{-1} during the titration (corresponding to a substantial enthalpic non-ideality parameter of 10 kJ mol^{-1}). Evaluation of the artificial data sets yielded an enthalpy close to the mean value, and K was recognized with an error of only 5%. Again, a combination of uptake and release experiments, which involve different variations in the membrane composition and are, therefore, differently affected by non-ideality effects, is a good test for the consistency and precision of the data obtained for real systems.

For a more detailed discussion and partitioning data for many systems, see papers on membrane binding of peptides [72, 80], surfactants [70, 81], alcohols [76, 82, 83] and drugs [84, 85] and references therein.

The apparent standard chemical potential change of a solute upon transfer from water into the lipid bilayer, $\Delta\hat{\mu}_S^{0,w\to b}$, is obtained as

$$\Delta\hat{\mu}_S^{0,w\to b} = -RT\ln(KC_W) \tag{11}$$

with the water concentration in dilute solutions, $C_W = 55.5$ M (for a detailed discussion, see [70]). The contribution of hydrophobic groups that are buried in the apolar core of the membrane to $\Delta\hat{\mu}_S^{0,w\to b}$ is similar to that obtained upon self-association to micelles (e.g., $\approx$3 kJ mol^{-1} per methylene). However, the enthalpy and heat capacity changes upon membrane insertion are quite different from those of micelle formation, indicating that changes in lipid packing caused by the solute may have substantial consequences.

Solute-into-lipid injections can be done in order to measure or confirm the enthalpy of membrane incorporation, $\Delta H_S^{w\to b}$, independently of K. This requires that the lipid concentration is sufficiently high ($C_L \gg K^{-1}$) to ensure that all solute is bound. Then, $\Delta C^{inj} = \Delta C^{trans}$ (see section 2.1, iii) and $Q - Q_{dil} = \Delta H_S^{w\to b}$.

4.3. Membrane binding of charged solutes, proteins and DNA

For charged solutes one has to take into account that the aqueous concentration of the solute in the vicinity of the membrane, which is in equilibrium with the membrane-bound solute, differs from that in the bulk solution, $C_S^{w,bulk}$. The *apparent partition coefficient* based on the bulk concentration, K^{app}, is strongly dependent on the electrostatic potential of the membrane surface with respect to the bulk, ψ_0, and the charge number of the solute, z_S:

$$K^{app} = \frac{C_S^b}{C_L C_S^{w,bulk}} = K^0 \exp\left\{-\frac{z_S e_0 N_A \psi_0}{RT}\right\} \tag{12}$$

with e_0 and N_A denoting the elementary charge and Avogadro's number, respectively. The potential depends, in turn, on the ionic strength and the bound solute, it can be numerically determined on the basis of Gouy–Chapman theory if the intrinsic partition coefficient, K^0, which does not depend on electrostatics, is to be determined [72, 86, 87].

The thermodynamics of ionization of a lipid upon addition of NaOH [88] and the adsorption of ions to lipid bilayers [89] were studied by ITC. A *variation in the buffer* used in ITC partitioning or binding experiments can be used to reveal protonation or deprotonation effects accompanying binding or membrane insertion of a ligand. This approach is based on the fact that protons released or bound by the ligand are absorbed or provided by the buffer, respectively, so that the heat of ionization of the buffer contributes to the heat of titration measured. Since the protonation heats of many buffers are known (see [90] and the appendix of [5]), the apparent heat of binding in different buffers can be plotted versus the heat of protonation of the buffers (figure 8), yielding the change in protonation (slope) and the intrinsic heat of binding (intercept) [72, 86, 91–95].

It should be noted that the assumption of a constant, average membrane surface potential (Gouy-Chapman Theory) is an approximation leading to good results in most cases. Nevertheless, one has to keep in mind that the local potential may be different, in particular for ligands that carry many charges. Charged ligands such as *peripheral proteins* exposing many positive charges towards the membrane surface may accumulate negatively charged lipids in a mixed membrane of anionic and zwitterionic lipids. Such effects have, for instance, been discussed in detail on the basis of ITC data on cytochrome C [96] and annexin/Ca^{2+} [97].

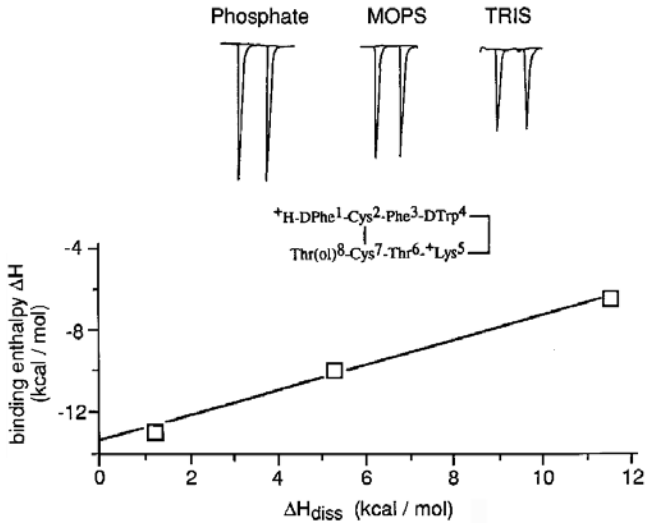

Figure 8. Buffer variation method to determine protonation/deprotonation effects accompanying membrane binding. The enthalpy of partitioning of the peptide ocreotide to POPC/POPG vesicles was measured by solute-into-lipid injections (section 4.2) in different buffers and the resulting $\Delta H_S^{w\to b}$ values were plotted versus the enthalpy of dissociation of the buffers. The slope implies that on average 0.63 protons are taken up by the peptide and the intercept indicates that $\Delta H_S^{w\to b}$ excluding heats of protonation is -13.4 kJ mol^{-1}. Reproduced with permission from [72], ©1997 Elsevier Science B.V.

The effects of polysaccharides on membrane properties were studied by DSC [98].

The binding of DNA to membranes containing cationic lipids has been characterized by ITC, revealing the thermodynamic parameters of the entropy-driven interaction as well as critical charge ratios [99] and protonation effects [95].

5. The effects of proteins and additives on membrane properties

5.1. Non-ideal mixing

The free energy of mixing in fluid membranes is often close to ideal since non-ideal enthalpic and entropic interactions and effects balance each other to a considerable extent (see next section). The enthalpy of mixing is, therefore, a much more sensitive parameter for investigating the non-ideal mixing behaviour of membrane constituents. We may write the enthalpy h of a system of two components, L and S, with X_S denoting the mole fraction of S, as

$$h = N_S H_S(1) + N_L H_L(0) + (N_L + N_S)\, H_E(X_S). \tag{13}$$

$H_S(1)$ and $H_L(0)$ stand for the molar enthalpies of S and L in pure systems. For ideal mixing, h is just a linear combination of the enthalpies of lipid and solute, and the excess enthalpy, H_E, vanishes. Non-ideal mixing is represented either by $H_E < 0$ if the S–L contacts are enthalpically favourable, or by $H_E > 0$ if S–L mixing is enthalpically unfavourable.

If the pure components are in only one state (and, for example, partitioning effects or CMCs can be neglected), $H_L(0)$ and $H_S(1)$ are constant (independent of the absolute concentration).

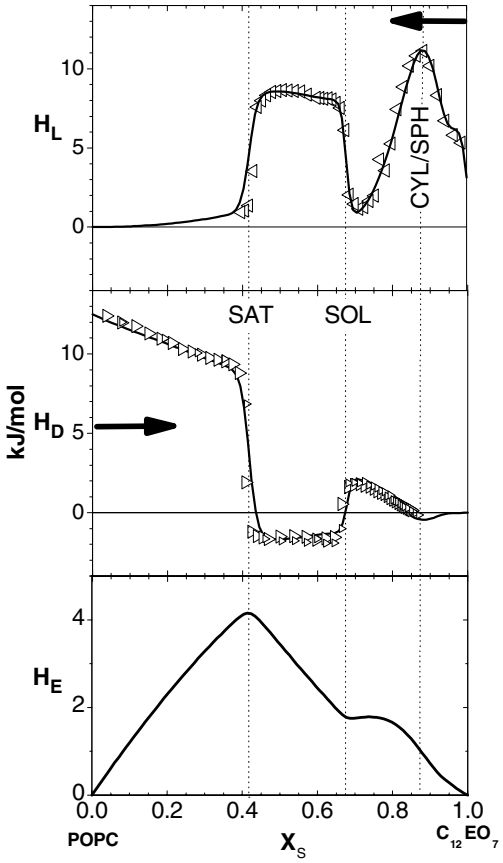

Figure 9. The partial molar enthalpies of the lipid, H_L, (top panel) and the micelle-forming detergent, H_D, (middle panel) in a mixture of POPC and $C_{12}EO_7$ measured by ITC (the data points in the top panel are measured from right to left). The solid curves fitted globally to H_L and H_D correspond to the same excess enthalpy function, $H_E(X)$ (bottom panel) according to equation (14) with $Q = H_L$ or $Q = H_D$, respectively. Break points indicate the onset (SAT) and completion (SOL) of the lamella-to-micelle transition (i.e., membrane solubilization, see section 5.6) and a cylinder-to-sphere transition of the micelles. Adapted from [100], ©1998 American Chemical Society.

The normalized heat, Q, of injection of a pure component (S or L) into the mixture was derived in [100], yielding

$$Q = (1 - X)\,\frac{\mathrm{d}H_E}{\mathrm{d}X} + H_E \tag{14}$$

with X denoting the mole fraction of the injectant (S or L) in the mixture (note that $X_L = 1 - X_S$ and $\mathrm{d}X_L = -\mathrm{d}X_S$). Hence, the heats measured upon titration of solute into lipid (middle panel of figure 9) and those measured upon titration of lipid into solute (top panel of figure 9) can be converted into each other or, independently, into one and the same excess enthalpy function, H_E, (bottom panel of figure 9) by solving equation (14). This was done for a series of lipid–detergent systems [100]. As one might expect, bilayer-forming additives show small, favourable or unfavourable non-ideality effects in lipid bilayers, but micelle-forming solutes (see figure 9) mix highly non-ideally with lipids in membranes, $H_E \gg 0$.

It is important to stress the difference between the *state* of the system (characterized by H_E) and the heat Q representing the partial molar enthalpy, i.e., the *trend* of the system upon addition of a substance. Positive values of Q do not necessarily mean that the mixing is unfavourable, but only that the addition of a compound renders the enthalpy of mixing less favourable.

The enthalpy of mixing in a membrane can also be studied by a detailed analysis of the shape of DSC curves of lipid transitions. Studies of lipid mixtures are discussed in section 3.2. Similar investigations have also been performed for *lipid–protein membranes* containing, for example, bacteriorhodopsin [101], cytochrome C [96, 102], gramicidin A [103] glycophorin [104] and tetanus toxin [105]. DNA binding can broaden and split the melting transition of cationic lipids [99].

5.2. Domain formation

The problem of whether molecules mix randomly or tend to form *clusters or domains* of certain compositions or arrangements is governed by the free energy. In fact, many lipid-additive systems showing strongly non-ideal enthalpies of mixing can nevertheless be well described as randomly arranged mixtures, since the endothermic enthalpies of interaction are essentially balanced by accompanying gains in entropy. The fact that many additives exhibit a virtually constant mole ratio partition coefficient (see (8)) into lipid bilayers [72, 81] implies slightly unfavourable excess free energies (defined analogously to (13)) of $G_E \leqslant 0.4\,\mathrm{kJ\,mol^{-1}}$ (see [70] for a detailed discussion). However, this non-ideality does not give rise to significant deviations from random mixing, since G_E is small compared to the thermal energy ($\approx$2.5 kJ mol^{-1} at room temperature).

Domains formed by spontaneous de-mixing of lipids in a membrane have recently become a focus of interest, since such domains in biological membranes, referred to as 'lipid rafts', are believed to have important biological functions. It has been assumed that these rafts can be isolated from the membranes by detergents. ITC studies of the enthalpy and entropy of interaction of the detergent triton with different lipids imply, however, that the addition of triton to the membrane changes the degree of domain formation and the composition of the domains substantially [106]. The predicted exothermic process of triton-induced formation or growth of domains could indeed by detected by ITC, and the stabilizing effect of triton on these domains could also be measured by DSC and PPC [26, 106].

5.3. The destabilization of membranes

Membrane *stability* can be directly quantified in terms of the free energy of the mixed membrane compared to the free energy of the most favourable alternative structure. For micelle-forming additives, the free energy of the alternative, micellar state can be approximated by that of pure additive micelles, since the freedom of micelles to vary their size and shape renders mixing in micelles typically close to ideal. Thus, the standard chemical potential difference of the solute between bilayers and micelles

$$\Delta\hat{\mu}_S^{0,b\to m} = RT \ln (K \cdot \mathrm{CMC}) \tag{15}$$

can be considered as an indicator for membrane destabilization by micelle-forming solutes [74]. Molecules perturbing the membrane already at low concentration show $\Delta\hat{\mu}_S^{0,b\to m} < 0$, i.e., $K \cdot \mathrm{CMC} < 1$. Molecules with $K \cdot \mathrm{CMC} > 1$ do not destabilize the membrane at low concentration but may solubilize membranes due to co-operative effects at very high additive concentrations.

Another approach to shed light on membrane-disordering effects of additives is to investigate their effect on the *melting temperature* T_m and other characteristics of the gel-to-liquid-crystalline transition of a model lipid. An additive that disorders the membrane can be expected to favour the fluid phase over the gel phase so that T_m is lowered (see, for example, [107, 108]).

5.4. Curvature strain in membranes

It has turned out that most of the membrane-ordering or -disordering effects of additives can be interpreted in terms of a relaxation or induction of curvature strain. The general background of these phenomena can most easily be illustrated by Israelachvili's concept of 'effective molecular shapes' (although molecules are, of course, flexible) [109]. Molecules such as POPC pack together to a planar arrangement since the surface area required by two fluid chains ($\approx 2 \times 27$ Å^2) agrees fairly well with the surface area occupied by the PC head group ($\approx$61–65 Å^2). Surfactants with a large head group but only one acyl chain are referred to as 'inverted cone-shaped'; they pack together to a strongly positively curved (i.e., convex), micellar surface. Molecules such as monoolein or DOPE, with a small head group and a hydrophobic part requiring a relatively large surface area, tend to form curved surfaces with the hydrated heads in the centre; these are called inverse or negatively curved structures. Whereas the preferred, 'spontaneous' or 'intrinsic' curvature varies gradually, the choice of surface curvatures that can be realized by stable aggregates is limited. The average real curvature of a lipid bilayer in a large vesicle is practically zero, but that of alternative (e.g., micellar) geometries differs substantially from zero. The difference between the spontaneous curvature of the constituents and the real curvature of the aggregate is called 'curvature strain'.

As a rule, enthalpies of membrane insertion of additives measured by ITC have been found to be the more endothermic the more curvature strain they create in a membrane [110, 111]. Additives that can relax a pre-existing curvature strain may bind exothermally [100, 110]. These results suggest that the excess enthalpy H_E of a bilayer (see section 5.2) is governed by the curvature strain.

Although non-ideal mixing and general membrane disordering are strongly related to curvature strain, a more specific interpretation of spontaneous curvature effects is possible considering the *lamellar-to-inverse hexagonal transition* of suitable model lipids (e.g., POPE) since the latter is accompanied by a real change in curvature from zero (lamellar) to negative values (inverse hexagonal). Compounds that induce positive spontaneous curvature favour the lamellar phase and increase the transition temperature, T_{hex}, whereas substances inducing negative spontaneous curvature promote the curved phase and decrease T_H [112–115]. Membrane curvature effects of compounds have been found to play an important role in biological membrane function [116–120].

5.5. Membrane permeabilization

The uptake into membranes of compounds that cannot undergo a fast flip from the outer to the inner lipid leaflet is limited by the constraint that both leaflets are coupled, having virtually the same lateral area. The threshold concentration at which an externally added, membrane impermeable compound breaks through to the inner monolayer has been discussed to cause a local minimum in the partial molar enthalpy of the compound in the membrane measured by ITC [75, 121, 122]. Pore formation in membranes by antibiotic peptides [123, 124] and the behaviour of cell-penetrating peptides such as TAT [125, 126] and penetratin [122, 127] have also been studied by ITC.

5.6. Membrane solubilization

ITC is an excellent method to study membrane solubilization, i.e., the lamella-to-micelle transition induced by surfactants [128] and the reconstitution of vesicles upon addition of lipid to a micellar lipid–surfactant system [73] (see figure 6); for a review, see [81]. The unmatched sensitivity of this method arises from the fact that it does not detect the lamellar or micellar *state per se* but the *trend* of the system to form micelles or vesicles (see [100] and discussion of equation (14)). Below the critical concentration for solubilization, injected surfactant micelles dissolve, and the surfactant is (at least partially) inserted into the membrane. This micelle-to-membrane transfer is typically endothermic (middle panel of figure 9). The appearance of the first stable mixed micelles in the system cannot be detected by structure methods since virtually all material is still lamellar. However, it reverses the direction of surfactant transfer; injected surfactant micelles persist now and extract surfactant (exothermic) and lipid from vesicles. This leads to a sudden jump (usually accompanied by a change in sign) of the heat of titration. If the experiment cannot be carried out under conditions where essentially all surfactant is membrane-bound, membrane–water partitioning must be taken into account when the critical surfactant-to-lipid ratios for the onset and completion of solubilization are determined [79, 106, 129]. The surfactant-induced lamella-to-micelle transition of lipid systems has also been studied by DSC [130].

The transition of fluid lipid bilayers to the inverse hexagonal phase can be induced by increasing temperature (monitored by DSC) or by the addition of compounds or changes in ionization inducing negative spontaneous curvature (studied by ITC, [131]).

5.7. Membrane fusion

The fusion of viruses with lipid vesicles has been studied using ITC [94, 132]. Since integral heats of titration do not provide any information on transient states, the heat of fusion of bilayers *per se* is small, and the heat effects observed should be mainly attributed to interactions of viral proteins with the target membrane. For example, a partial deprotonation of a viral protein upon membrane fusion was detected by ITC using the buffer variation method (see section 4.3) [94]. The enthalpy of proton-induced vesicle fusion was measured by ITC [131]. DSC studies of viral proteins have yielded important information on fusogenic protein states in viruses (next section).

6. The effects of membranes on proteins

6.1. The stability of proteins in a membrane environment

The denaturation behaviour of membrane proteins has been studied by DSC in reconstituted vesicles as well as in whole viruses or cells; for a review, see [133]. To mention but a few examples, Epand *et al* [134] found a stabilizing effect of glucose on a transmembrane glucose transporter, GLUT1, in an endogenous lipid environment. The addition of salt changes the denaturation behaviour of membrane-reconstituted yeast cytochrome C oxidase [69]. Cholesterol enhances the stability of rhodopsin in intact disc membranes and reconstituted membranes, and shifts the equilibrium between the different conformational states (see [135] and references therein). The influence of anaesthetics on the thermal stability of proteins in erythrocyte and sarcoplasmatic reticulum membranes was studied in order to elucidate the effect of anaesthetics sensitizing cells to hyperthermia [136].

DSC of various viruses was done to characterize the thermal denaturation of viral proteins and shed light on the effects governing viral fusion [137–139]. The ‘spring-loaded trap’ model

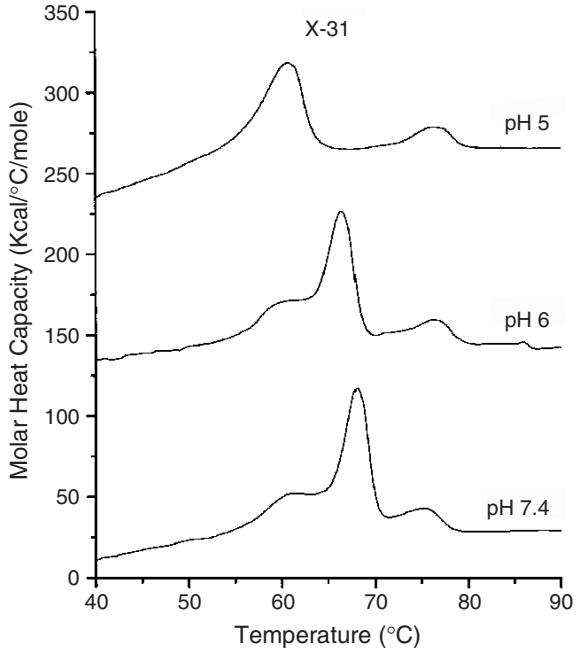

Figure 10. DSC curves of influenza virus. The largest peak could be assigned to the thermal denaturation of haemagglutinin. Reproduced with permission from [139], ©2002 Biochemical Society.

of viral fusion assumes that haemagglutinin, HA, is in a high-energy metastable state at neutral pH, but a DSC study of the whole virus showed endotherms of partial denaturation of HA and other proteins rather than an exothermic process indicative of relaxing a kinetically entrapped 'spring' (figure 10, [139]).

Most membrane proteins seem to exhibit smaller enthalpies of denaturation ($\approx$14 kJ g^{-1}) than typical soluble proteins ($\approx$33 kJ g^{-1}), suggesting that the membrane stabilizes some residual structure (see [139] and references therein). Marked differences between the denaturation behaviour of HA in viral membranes compared to isolated HA illustrate the importance of the specific membrane environment for the stability and function of membrane proteins [139].

6.2. The membrane-assisted folding of peptides

Hydrophobic stretches of proteins may form α-helices within the membrane, with thermodynamics ruled by both hydrophobic interactions and helix formation. Peptides such as mellitin or magainin contain charged and hydrophobic amino acids and are soluble in the random coil state in buffer. Upon partitioning into a membrane, they form an amphipathic α-helix with charged and polar residues lined up on one side of the helix and hydrophobic amino acids on the other. Hence, the hydrophobic side chains can insert into an apolar membrane environment, whereas the charged amino acids remain exposed to water. Again, membrane partitioning and helix formation are coupled. Wieprecht *et al* [140, 141] could separate the two effects by ITC experiments comparing all-L peptides with DD-isomers which should show the same hydrophobicity but are not (or are less) capable of forming a helical structure. They established that helix formation at the membrane surface is characterized by

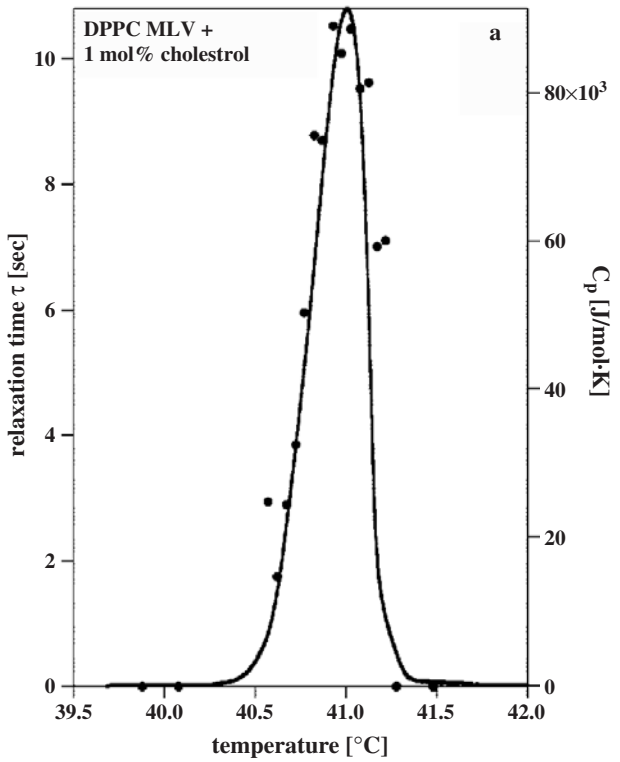

Figure 11. Relaxation times of chain melting in DPPC vesicles containing 1 mol% of cholesterol as measured by pressure-jump calorimetry (●, left-hand ordinate) and the corresponding heat capacity profile obtained by DSC (——, right-hand ordinate). Reproduced with permission from [18], ©2002 American Biophysical Society.

$\Delta\Delta H \approx -0.7$ kcal mol^{-1}, $\Delta\Delta S^0 \approx -1.9$ cal mol^{-1}K^{-1}, and $\Delta\Delta G^0 \approx -0.14$ kcal mol^{-1}, all given per residue.

7. Kinetics

Detailed studies of the kinetics of lipid phase transitions in the absence and presence of additives have been performed by measuring the time-dependent thermal response of lipid samples to periodic pressure modulations [19, 20, 22] and pressure jumps [17, 18]. Figure 11 illustrates the relationship between the temperature-dependent relaxation times of chain melting and the heat capacity. Small amounts (1 mol%) of cholesterol added to DPPC reduce the relaxation time, τ, by a factor of 4 [18] whereas 1.3 mol% of the anesthetic dibucaine increase τ two-fold [21]. These effects are related to the size of cooperatively melting clusters in the membranes.

Information on kinetics and activation energies of transitions can also be obtained by investigating the effect of the DSC scan rate on the apparent transition temperature and the shape of the DSC peaks [9, 134].

ITC provides information on the kinetics of re-equilibration after injections [69]. Membrane partitioning of solutes is often fast compared to the time constant of fast calorimeters ($\approx$15 s). If the penetration of the solute to the inner monolayer occurs within a few minutes, the heat peaks may exhibit a biphasic behaviour [75]. Water sorption calorimetry with sudden,

small changes in RH reveals the swelling to occur within about ten minutes if the film is thin enough and the gas flow is sufficiently fast (see figure 2); an interpretation in terms of system kinetics is hardly possible.

Even if kinetic constants are not of particular interest, it must be guaranteed for a thermodynamic evaluation of the data that the system reaches equilibrium during the experiment. For example, the next injection of an ITC run should only be made after sufficient time for the heat response to reach the baseline level. It must, however, be stressed that this is a necessary but not sufficient criterion for having reached equilibrium, since the re-equilibration of the system after an injection may exhibit complex kinetics with slow processes following fast ones. In most cases, there is a simple but very effective means to rule out problems arising from slow processes: to combine up- and down-scans or scans with different speed. This is routine in the DSC of lipids. In ITC, it is advisable to combine, for example, uptake and release or solubilization and reconstitution experiments to rule out incomplete equilibration. In sorption calorimetry, it is useful to compare up- and down-scans in RH. PPC performs up- and down-jumps in pressure routinely, thus allowing one to recognize irreversible effects and metastable states occurring upon a transition [142].

Acknowledgments

I thank Thomas Heimburg, Sandro Keller and Alekos Tsamaloukas for important comments on the manuscript. Financial support from the Swiss National Science Foundation (grant 31-67216.01) is gratefully acknowledged.

Appendix A. The derivation of equation (9)

A model describing the ITC uptake as well as the release assay can be derived as follows. The concentration of membrane-bound solute C_S^b is written as

$$C_S^b = C_S \phi \tag{16}$$

with the membrane-bound fraction of the solute, ϕ

$$\phi \equiv \frac{C_S^b}{C_S} = \frac{K C_L}{1 + K C_L}, \tag{17}$$

which varies between $\phi = 0$ for the case that all solute is in aqueous solution and $\phi = 1$ for complete partitioning into the membrane. The expression for ϕ in terms of K and C_L is derived from the definition of the partition coefficient, equation (8), taking into account the conservation of mass, $C_S^w = C_S - C_S^b$.

Both uptake and release assays agree in that the cell contains no lipid before the first injection, but the solute is either filled into the cell prior to the titration (concentration C_S^{ini}, uptake) or it comes with the lipid in a proportion given by the mole ratio of solute per lipid in the syringe, $R^{syr} = C_S^{syr}/C_L^{syr}$ (release). Generally, we may write

$$C_S = C_S^{ini} + R^{syr} C_L. \tag{18}$$

Note that different corrections for overflowing cell contents may apply to C_S^{ini} and C_L depending on the instrument used (not shown here). The increase in C_S^b in the cell per mole of lipid injected is obtained by differentiating (16):

$$\frac{dC_S^b}{dC_L} = \frac{d(\phi C_S)}{dC_L} = \phi' C_S + \phi R^{syr} \tag{19}$$

with $dC_S/dC_L = R^{syr}$ obtained by differentiation of (18). ϕ' is derived by differentiation of (17):

$$\phi' = \frac{d\phi}{dC_L} = \frac{K}{(1 + KC_L)^2}. \tag{20}$$

Equation (19) with (20) specifies the change in the concentration of membrane-bound solute in the cell. This includes, first, the solute that is binding from water to the membrane within the cell, which is the source of the observed heat. Second, it includes solute that was already bound when it was injected into the cell along with lipid; this part does not yield any heat of binding. The total injected solute is $R^{syr}\,dC_L$ (see (18)) and thus, the pre-bound, injected solute is $\phi^{syr}R^{syr}\,dC_L$ with ϕ^{syr} being defined analogously to (17) for the syringe content. Hence, for deriving the heat-producing solute per lipid injected, see dC^{trans}/dC^{inj} in equation (3), we have to subtract the enthalpically silent addition of pre-bound solute, which is just $\phi^{syr}R^{syr}$, from dC_S^b/dC_L in (19), yielding

$$Q = \left[\phi'\left(C_S^{ini} + R^{syr}C_L\right) - \left(\phi^{syr} - \phi\right)R^{syr}\right]\Delta H_S^{w\to b} + Q_{dil} \tag{21}$$

which yields the fit function (9) after insertion of $\phi(K)$ and $\phi'(K)$ (equations (17), (20)).

Appendix B. Response to Randzio's comments on PPC [24]

All issues raised by Randzio in [24] are discussed in the following.

(1) [24] stresses that the instrument works in a constant-volume mode so that the mass, m, of the sample within the cell changes upon a pressure jump. The subsequent relative change is $\Delta m/m = 2.5 \times 10^{-4}$ (based on the compressibility of water, $\kappa \approx 5 \times 10^{-10}$ Pa^{-1}, and the pressure change, $\Delta P \approx \pm 5 \times 10^5$ Pa). Since the mass change is fast compared to the detection of the heat, the heat detected after a pressure decrease corresponds to the correct mass of water (at ambient pressure) and the heat measured upon pressure increase would be by 0.025% too large, which is clearly irrelevant.

(2) [24] criticizes that the coefficient of isobaric volume expansion, α_p, and the molar volume, V_m, would be assumed to be invariant with pressure. Pressure-dependent values of α for hexane and ethyl alcohol [14] suggest a maximum slope of 10^{-6} K^{-1} bar^{-1} at low pressure. If similar values apply to other compounds, the variation of α_p upon a 5 bar jump is $\approx 5 \times 10^{-6}$ K^{-1} (typically about 0.5%). The volume change of an aqueous solution is 0.03% as mentioned above. Hence, it is an excellent approximation to assume α_p, V_m = constant under these conditions.

(3) [24] stresses that the data evaluation would not distinguish between the partial volume of the solute and the cell volume, referring to equation (4) in [143]. This equation belongs to a section entitled 'single component systems' where such a distinction is obviously not appropriate. The next section, entitled 'two-component systems', gives a detailed description of the partial volume changes of the solute.

(4) [24] argues against observing finite α values at the phase transition temperature, since the theory of first-order transitions implies that α is discontinuous at this temperature. The problem is perfectly equivalent to the fact that DSC curves show finite C_p values at transition temperatures. However, this does not mean that DSC or PPC curves are useless or wrong, but illustrates the fact that experimental data of real samples may deviate from the theory of ideal systems.

(5) [24] notes that heat effects may arise from differences in the active volume and mechanic properties of the sample and reference cell. This is indeed the case. These heats are measured by blank experiments filling both cells with water or buffer (yielding small, virtually identical heats) and automatically subtracted from every experimental data set.

(6) [24] claims that the experimental process would be adiabatic rather than isothermal, since the pressure change is faster than the heat response of the instrument. This may be true but would, again, not be relevant, since a slight delay in compensating local temperature deviations in the centre of the cell does not affect the amount of the compensation heat integrated over time until equilibrium is reached, usually in less than a minute.

References

[1] Cevc G and Marsh D 1985 *Phospholipid Bilayers* (New York: Wiley)
[2] Cevc G 1993/2004 *Phospholipids Handbook* (New York: Dekker)
[3] Lipowsky R and Sackmann E 1995 *Structure and Dynamics of Membranes* (Amsterdam: Elsevier Science B.V.)
[4] Ladbury J E and Doyle M L 2003 *Biocalorimetry* vol 2 (New York: Wiley)
[5] Haynie D 2001 *Biological Thermodynamics* (Cambridge: Cambridge University Press)
[6] Wadsö I 1997 *Chem. Soc. Rev.* **26** 79–86
[7] Lin L N, Brandts J F, Brandts J M and Plotnikov V 2002 *Anal. Biochem.* **302** 144–60
[8] Lerchner J, Wolf A and Wolf G 1999 *J. Therm. Anal. Calorim.* **57** 241–51
[9] Leharne S A and Chowdhry B Z 1998 *Biocalorimetry* ed J Ladbury and B Z Chowdhry (Chichester: Wiley) pp 157–82
[10] Plotnikov V V, Brandts J M, Lin L N and Brandts J F 1997 *Anal. Biochem.* **250** 237–44
[11] Privalov G, Kavina V, Freire E and Privalov P L 1995 *Anal. Biochem.* **232** 79–85
[12] Blume A 1983 *Biochemistry* **22** 5436–42
[13] Heerklotz H 1998 *Biocalorimetry* ed J Ladbury and B Chowdhry (Chichester: Wiley) pp 89–100
[14] Pruzan P, Minassian L T, Figuiere P and Szwarc H 1976 *Rev. Sci. Instrum.* **47** 66–71
[15] Randzio S L 1997 *J. Therm. Anal.* **48** 573–83
[16] Randzio S L, Grolier J P E and Quint J R 1994 *Rev. Sci. Instrum.* **65** 960–5
[17] Heimburg T, Grabitz P and Ivanova V P 2001 *Biophys. J.* **80** 2148
[18] Grabitz P, Ivanova V P and Heimburg T 2002 *Biophys. J.* **82** 299–309
[19] Johnson M L, van Osdol W W and Biltonen R L 1986 *Methods Enzymol.* **130** 534–51
[20] van Osdol W W, Johnson M L, Ye Q and Biltonen R L 1991 *Biophys. J.* **59** 775–85
[21] van Osdol W W, Ye Q, Johnson M L and Biltonen R L 1992 *Biophys. J.* **63** 1011–7
[22] Chen L, Biltonen R L and Johnson M L 1995 *Energetics of Biological Macromolecules* pp 169–82
[23] Heerklotz H and Seelig J 2002 *Biophys. J.* **82** 1445–52
[24] Randzio S L 2003 *Thermochim. Acta* **398** 75–80
[25] Ebel H, Grabitz P and Heimburg T 2001 *J. Phys. Chem.* B **105** 7353–60
[26] Heerklotz H 2002 *Biophys. J.* **83** 2693–701
[27] Bakri A 1993 *ThermoMetric Application Note* http://www.thermometric.com/pdf/an22021.pdf (22021)
[28] Binder H, Kohlstrunk B and Heerklotz H H 1999 *J. Colloid Interface Sci.* **220** 235–49
[29] Binder H, Kohlstrunk B and Heerklotz H H 1999 *Chem. Phys. Lett.* **304** 329–35
[30] Humivar http://www.humivar.de
[31] Smith A L, Shirazi H M and Mulligan S R 2002 *Biochim. Biophys. Acta* **1594** 150–9
[32] Masscal www.masscal.com
[33] Markova N, Sparr E, Wadso L and Wennerstrom H 2000 *J. Phys. Chem.* B **104** 8053–60
[34] Markova N, Sparr E and Wadso L 2001 *Thermochim. Acta* **374** 93–104
[35] Nebel S, Ganz P and Seelig J 1997 *Biochemistry* **36** 2853–9
[36] Ladbrooke B D and Chapman D 1969 *Chem. Phys. Lipids* **3** 304–56
[37] Chapman D and Urbina J 1974 *J. Biol. Chem.* **249** 2512–21
[38] Koynova R and Caffrey M 1994 *Chem. Phys. Lipids* **69** 181–207
[39] Koynova R and Caffrey M 1994 *Chem. Phys. Lipids* **69** 1–34
[40] Koynova R and Caffrey M 1995 *Biochim. Biophys. Acta* **1255** 213–36
[41] Koynova R and Caffrey M 1998 *Biochim. Biophys. Acta* **1376** 91–145
[42] LIPIDAT http://www.lipidat.chemistry.ohio-state.edu
[43] Bottner M and Winter R 1993 *Biophys. J.* **65** 2041–6
[44] Lee A G 1977 *Biochim. Biophys. Acta* **472** 285–344
[45] Johann C, Garidel P, Mennicke L and Blume A 1996 *Biophys. J.* **71** 3215–28
[46] McMullen T P, Lewis R N and McElhaney R N 1993 *Biochemistry* **32** 516–22
[47] McMullen T P W and McElhaney R N 1995 *Biochim. Biophys. Acta—Biomembr.* **1234** 90–98

[48] Blume A 1980 *Biochemistry* **19** 4908–13
[49] Vist M R and Davis J H 1990 *Biochemistry* **29** 451–64
[50] Nyholm T K, Nylund M and Slotte J P 2003 *Biophys. J.* **84** 3138–46
[51] Mannock D A, McIntosh T J, Jiang X, Covey D F and McElhaney R N 2003 *Biophys. J.* **84** 1038–46
[52] Winter R 2001 *Curr. Opin. Colloid Interface Sci.* **6** 303–12
[53] Mountcastle D B, Biltonen R L and Halsey M J 1978 *Proc. Natl Acad. Sci. USA* **75** 4906–10
[54] Landwehr A and Winter R 1994 *Ber. Bunsenges. Phys. Chem.* **98** 214–8
[55] Prasad S K, Shashidhar R, Gaber B P and Chandrasekhar S C 1987 *Chem. Phys. Lipids* **43** 227–35
[56] Parsegian V A and Rand R P 1995 *Handbook of Biological Physics* ed RLaE Sackmann (Amsterdam: Elsevier Science B.V.) pp 644–88
[57] Israelachvili J and Wennerstrom H 1996 *Nature* **379** 219–25
[58] Binder H, Kohlstrunk B and Pohle W 2000 *J. Phys. Chem.* B **104** 12049–55
[59] Pfeiffer H, Binder H, Klose G and Heremans K 2003 *Biochim. Biophys. Acta—Biomembr.* **1609** 148–52
[60] Takahashi H, Aoki H, Inoue H, Kodama M and Hatta I 1998 *Thermochim. Acta* **308** 85–91
[61] Kodama M, Aoki H, Takahashi H and Hatta I 1997 *Biochim. Biophys. Acta—Biomembr.* **1329** 61–73
[62] Ollivon M R 1991 *Adv. Exp. Med. Biol.* **302** 175–89
[63] Heerklotz H and Epand R M 2001 *Biophys. J.* **80** 271–9
[64] Chellani M 1999 *Am. Biotechnol. Lab.* **17** 14–18
[65] Lin L N, Li J Y, Brandts J F and Weiss R M 1994 *Biochemistry* **33** 6564–70
[66] Machaidze G, Ziegler A and Seelig J 2002 *Biochemistry* **41** 1965–71
[67] Wenk M R and Seelig J 1997 *Biophys. J.* **73** 2565–74
[68] Heerklotz H H, Binder H and Epand R M 1999 *Biophys. J.* **76** 2606–13
[69] Morin P E and Freire E 1991 *Biochemistry* **30** 8494–500
[70] Heerklotz H 2004 *Phospholipids Handbook* ed G Cevc (New York: Plenum)
[71] Seelig J and Ganz P 1991 *Biochemistry* **30** 9354–9
[72] Seelig J 1997 *Biochim. Biophys. Acta* **1331** 103–16
[73] Heerklotz H, Lantzsch G, Binder H, Klose G and Blume A 1996 *J. Phys. Chem.* **100** 6764–74
[74] Heerklotz H and Seelig J 2000 *Biophys. J.* **78** 2435–40
[75] Heerklotz H 2001 *Biophys. J.* **81** 184–95
[76] Zhang F and Rowe E S 1992 *Biochemistry* **31** 2005–11
[77] Rowe E S, Zhang F, Leung T W, Parr J S and Guy P T 1998 *Biochemistry* **37** 2430–40
[78] Opatowski E, Kozlov M M and Lichtenberg D 1997 *Biophys. J.* **73** 1448–57
[79] Keller M, Kerth A and Blume A 1997 *Biochim. Biophys. Acta* **1326** 178–92
[80] Wieprecht T and Seelig J 2002 *Peptide–Lipid Interactions* (*Current Topics in Membranes* vol 52) (New York: Academic) pp 31–56
[81] Heerklotz H and Seelig J 2000 *Biochim. Biophys. Acta* **1508** 69–85
[82] Westh P, Trandum C and Koga Y 2001 *Biophys. Chem.* **89** 53–63
[83] Suurkuusk M and Singh S K 1998 *Chem. Phys. Lipids* **94** 119–38
[84] Wenk M R, Fahr A, Reszka R and Seelig J 1996 *J. Pharm. Sci.* **85** 228–31
[85] Bauerle H D and Seelig J 1991 *Biochemistry* **30** 7203–11
[86] Beschiaschvili G and Seelig J 1992 *Biochemistry* **31** 10044–53
[87] Terzi E, Holzemann G and Seelig J 1994 *Biochemistry* **33** 7434–41
[88] Blume A and Tuchtenhagen J 1992 *Biochemistry* **31** 4636–42
[89] Lehrmann R and Seelig J 1994 *Biochim. Biophys. Acta* **1189** 89–95
[90] Fukada H and Takahashi K 1998 *Proteins Struct. Funct. Genet.* **33** 159–66
[91] Flogel M and Biltonen R L 1975 *Biochemistry* **14** 2610–5
[92] Seelig J, Nebel S, Ganz P and Bruns C 1993 *Biochemistry* **32** 9714–21
[93] Baker B M and Murphy K P 1996 *Biophys. J.* **71** 2049–55
[94] Ravoo B J, Weringa W D and Engberts J 2000 *Cell Biol. Int.* **24** 787–97
[95] Lobo B A, Koe G S, Koe J G and Middaugh C R 2003 *Biophys. Chem.* **104** 67–78
[96] Heimburg T, Angerstein B and Marsh D 1999 *Biophys. J.* **76** 2575–86
[97] Patel D R, Jao C C, Mailliard W S, Isas J M, Langen R and Haigler H T 2001 *Biochemistry* **40** 7054–60
[98] Steffan G, Wulff S and Galla H J 1994 *Chem. Phys. Lipids* **74** 141–50
[99] Barreleiro P C A, Olofsson G and Alexandridis P 2000 *J. Phys. Chem.* B **104** 7795–802
[100] Heerklotz H H, Binder H and Schmiedel H 1998 *J. Phys. Chem.* B **102** 5363–8
[101] Heyn M P, Blume A, Rehorek M and Dencher N A 1981 *Biochemistry* **20** 7109–15
[102] Heimburg T and Biltonen R L 1994 *Biochemistry* **33** 9477–88
[103] Ivanova V P, Makarov I M, Schaffer T E and Heimburg T 2003 *Biophys. J.* **84** 2427–39

[104] Tampe R, von Lukas A and Galla H J 1991 *Biochemistry* **30** 4909–16
[105] Winter A, Ulrich W P, Wetterich F, Weller U and Galla H J 1996 *Chem. Phys. Lipids* **81** 21–34
[106] Heerklotz H, Szadkowska H, Anderson T and Seelig J 2003 *J. Mol. Biol.* **329** 793–9
[107] Lohner K, Latal A, Lehrer R I and Ganz T 1997 *Biochemistry* **36** 1525–31
[108] Prenner E J, Lewis R, Kondejewski L H, Hodges R S and McElhaney R N 1999 *Biochim. Biophys. Acta—Biomembr.* **1417** 211–23
[109] Israelachvili J N 1991 *Intermolecular and Surface Forces* (London: Academic)
[110] Epand R M and Epand R F 1994 *Biophys. J.* **66** 1450–6
[111] Heerklotz H, Binder H, Lantzsch G, Klose G and Blume A 1997 *J. Phys. Chem.* B **101** 639–45
[112] Liu F, Lewis R, Hodges R S and McElhaney R N 2001 *Biochemistry* **40** 760–8
[113] Epand R M, Epand R F and Lancaster C R 1988 *Biochim. Biophys. Acta* **945** 161–6
[114] Foht P J, Tran Q M, Lewis R and McElhaney R N 1995 *Biochemistry* **34** 13811–7
[115] Hallock K J, Lee D K and Ramamoorthy A 2003 *Biophys. J.* **84** 3052–60
[116] Gruner S M 1985 *Proc. Natl Acad. Sci. USA* **82** 3665–9
[117] Wieslander A, Christiansson A, Rilfors L, Khan A, Johansson L B and Lindblom G 1982 *Rev. Infect. Dis.* **4** (Suppl) S43–9
[118] Bhakoo M and McElhaney R N 1988 *Biochim. Biophys. Acta* **945** 307–14
[119] Giorgione J R, Kraayenhof R and Epand R M 1998 *Biochemistry* **37** 10956–60
[120] Davies S M, Epand R M, Kraayenhof R and Cornell R B 2001 *Biochemistry* **40** 10522–31
[121] Hildebrand A, Neubert R, Garidel P and Blume A 2002 *Langmuir* **18** 2836–47
[122] Binder H and Lindblom G 2003 *Biophys. J.* **85** 982–95
[123] Wieprecht T, Apostolov O, Beyermann M and Seelig J 2000 *Biochemistry* **39** 442–52
[124] Wenk M R and Seelig J 1998 *Biochemistry* **37** 3909–16
[125] Ziegler A, Blatter X L, Seelig A and Seelig J 2003 *Biochemistry* **42** 9185–94
[126] Ziegler A and Seelig J 2004 *Biophys. J.* **86** 254–63
[127] Binder H and Lindblom G 2003 *Phys. Chem. Chem. Phys.* **5** 5108–17
[128] Heerklotz H, Lantzsch G, Binder H, Klose G and Blume A 1995 *Chem. Phys. Lett.* **235** 517–20
[129] Wenk M R and Seelig J 1997 *J. Phys. Chem.* B **101** 5224–31
[130] Majhi P R and Blume A 2002 *J. Phys. Chem.* B **106** 10753–63
[131] Wenk M R and Seelig J 1998 *Biochim. Biophys. Acta—Biomembr.* **1372** 227–36
[132] Nebel S, Bartoldus I and Stegmann T 1995 *Biochemistry* **34** 5705–11
[133] Shnyrov V L, SanchezRuiz J M, Boiko B N, Zhadan G G and Permyakov E A 1997 *Thermochim. Acta* **302** 165–80
[134] Epand R F, Epand R M and Jung C Y 1999 *Biochemistry* **38** 454–8
[135] Albert A D, Boesze-Battaglia K, Paw Z, Watts A and Epand R M 1996 *Biochim. Biophys. Acta* **1297** 77–82
[136] Senisterra G A and Lepock J R 2000 *Int. J. Hyperth.* **16** 1–17
[137] Shnyrov V L, Zhadan G G, Cobaleda C, Sagrera A, MunozBarroso I and Villar E 1997 *Arch. Biochem. Biophys.* **341** 89–97
[138] Rexroad J, Wiethoff C M, Green A P, Kierstead T D, Scott M O and Middaugh C R 2003 *J. Pharm. Sci.* **92** 665–78
[139] Epand R M and Epand R F 2002 *Biochem. J.* **365** 841–8
[140] Wieprecht T, Apostolov O, Beyermann M and Seelig J 1999 *J. Mol. Biol.* **294** 785–94
[141] Wieprecht T, Beyermann M and Seelig J 2002 *Biophys. Chem.* **96** 191–201
[142] Wang S L and Epand R M 2004 *Chem. Phys. Lipids* **129** 21–30
[143] Kujawa P and Winnik F M 2001 *Macromolecules* **34** 4130–5